AIAA 81-0626R

A Hybrid State Vector Approach to Aeroelastic Analysis

Larry L. Lehman*
Nielsen Engineering & Research, Inc., Mountain View, California

A computational technique has been developed for performing preliminary design aeroelastic analyses of large-aspect-ratio lifting surfaces. This technique, applicable to both fixed and rotating wing configurations, is based upon a formulation of the structural equilibrium equations in terms of a hybrid state vector containing generalized force and displacement variables. An integrating matrix is employed to solve these equations for divergence and flutter eigenvalues and steady aeroelastic deformation. Results are presented for simple examples that verify the technique and demonstrate how it can be applied to analyze lifting surfaces, including those constructed from composite materials.

Nomenclature

$A, \tilde{A}$ = local, global matrix expressing displacement dependent loads
A^*, B^*, D^* = dimensional composite plate compliance matrices
$\tilde{A}^*_{ij}, \tilde{B}^*_{ij}, \tilde{D}^*_{ij}$ = nondimensional composite plate compliance terms $(i,j = 1,2,3)$
$a_r, \tilde{a}_r$ = local, global vector of loads for a rigid structure
B_n = boundary condition matrix for point n
$b, \tilde{b}$ = dimensional, nondimensional aerodynamic semichord, $\tilde{b} = b/b_R$
C, C_{FD} = matrix, submatrix containing structural damping terms
c = chord length of structural box normal to structural reference axis
D = constant matrix defined by Eqs. (3) and (6)
D_{ij} = element of composite plate bending stiffness matrix
EI = bending stiffness
GJ = torsional stiffness
I = identity matrix
K = symmetric matrix containing structural terms, defined by Eq. (3)
$\tilde{k}$ = constant vector of integration
$L, \tilde{L}$ = local, global integrating matrix (type one)
L^* = integrating matrix (type two)
ℓ = semispan length
m = dimensional vector of moment resultants
M, M_{FD} = matrix, submatrix containing mass terms
$M_i, \tilde{M}_i$ = dimensional, nondimensional components of moment resultant vector, $i = x,y,xy$
$m, \tilde{m}$ = dimensional, nondimensional running mass, $\tilde{m} = m/m_R$
n = dimensional vector of stress resultants
$N_i, \tilde{N}_i$ = dimensional, nondimensional components of stress resultant vector, $i = x,y,xy$
n = number of discretization points
p = vector of running external loads
$p_i, \tilde{p}_i$ = dimensional, nondimensional running external loads for ith degree of freedom, $i = u,\gamma,w,\alpha$
Q, Q_{FD} = matrix, submatrix containing unsteady aerodynamic terms
q = dynamic pressure
$\tilde{r}_\alpha$ = nondimensional section radius of gyration, $\tilde{r}_\alpha = r_\alpha/b_R$
$\tilde{S}^*$ = nondimensional transverse shear compliance
s, s^* = dimensional, nondimensional Laplace variable
$\mathfrak{U}$ = functional in Eq. (1)
$V_x, \tilde{V}_x$ = dimensional, nondimensional transverse shear resultant
u, v, w = spanwise, streamwise, and vertical displacements
$\tilde{u}, \tilde{v}, \tilde{w}$ = nondimensional spanwise, streamwise, and vertical displacements, nondimensionalized by ℓ
x, y, z = spanwise, streamwise, and vertical coordinates
$\tilde{x}, \tilde{y}, \tilde{z}$ = nondimensional spanwise, streamwise, and vertical coordinates, nondimensionalized by ℓ
$y, \tilde{y}$ = local, global state vector
$\hat{y}$ = Laplace transform of state vector
$Z, \tilde{Z}$ = local, global coefficient matrix containing structural terms
α = angle of twist (elastic angle of attack)
β = linear taper factor appearing in Eq. (A3)
β_s = dimensional transverse shear compliance
γ = rotation of normal to elastic axis
δ = first variation operator
ϵ^0 = vector of plate midplane strains
θ = composite fiber orientation angle (with respect to structural reference axis)
κ = vector of plate bending curvatures
λ = nondimensional dynamic pressure
Λ = wing sweep angle, positive aft
μ = mass ratio, $\mu = m_R/\pi\rho b_R^2$
ν = nondimensional dynamic pressure defined in Eqs. (A3) and (A4)
$\tilde{\chi}_\alpha$ = nondimensional section static unbalance, $\tilde{\chi}_\alpha = \chi_\alpha/b_R$
$(\ )'$ = $\mathrm{d}/\mathrm{d}x$ or $\mathrm{d}/\mathrm{d}\tilde{x}$
$(\ )^T$ = transpose
$\hat{}(\ )$ = diagonal matrix
$(\ )_D$ = displacement subset
$(\ )_F$ = force subset
$(\ )_i$ = evaluated at ith location
$(\ )_R$ = reference value

Presented as Paper 81-0626 at the AIAA Dynamic Specialists Conference, Atlanta, Ga., April 9-10, 1981; submitted April 24, 1981; revision received Jan. 4, 1982.

*Research Scientist. Member AIAA.

Introduction

An expanded utilization of laminated composite materials in aircraft structural design has led to a search for new ways to employ these lightweight materials efficiently. One result of this search has been the development of the concept of aeroelastic tailoring of a lifting surface, in which the directional characteristics of the composite material are used to synthesize a structure with enhanced aeroelastic performance. The purpose of this paper is to present a computational technique for performing the analyses required to

synthesize an aeroelastically tailored design for large-aspect-ratio lifting surfaces. The technique is based upon a formulation of the structural equilibrium equations in terms of a hybrid state vector containing both generalized force and displacement variables. An integrating matrix technique is then used to discretize and solve these equations for divergence and flutter eigenvalues and aeroelastic lift distribution.

Historically, most aeroelastic analyses of composite structures have been performed with the aid of very complex computer codes involving finite element structural methods coupled with lifting surface aerodynamics. Unfortunately, these complicated numerical approaches often tend to obscure a basic understanding of the important parameters appearing in the analysis and, owing to cost considerations, often preclude an extensive study involving numerous design variations. Recent developments such as those of Gimmestad,[1] however, have progressed toward more efficient analysis routines that are suitable for preliminary design investigations.

A fundamental approach to performing the aeroelastic analyses for a structure that can be appropriately described in terms of one independent spatial coordinate involves formulating the differential equations representing the aeroelastic response and obtaining analytical solutions to the resulting boundary-value problems. Although the coupled bending and torsion equations can be formulated, it is often difficult, if not impossible, to obtain analytical solutions for the general case in which the coefficients are variable. Some useful solutions have been obtained, however, for cases in which the coefficients in the linear aeroelastic equations can be written as constants. For instance, solutions for divergence and load distribution have been obtained for isotropic metallic wings by Diederich and Budiansky[2] and Diederich and Foss.[3] More recently, Weisshaar[4,5] has examined divergence and load distribution for composite swept-forward wings. With the application of the state vector approach presented herein, approximate solutions to the differential equations have been easily obtained for the more difficult cases involving variable coefficients. This type of solution does not require an explicit calculation of structural influence coefficients, and can utilize any form of aerodynamic influence matrix.

Structural Equilibrium Equations

Variational Formulation

A general formulation of the structural equations is presented here which casts them into a state vector form involving a coupled system of first-order differential equations. Although this type of formulation is not entirely new to structural mechanics, it has never seen extensive practical use; however, recent investigations by Steele,[6] Steele et al.,[7] and Steele and Barry[8] have indicated that it can be advantageous for both analysis and numerical calculation. A variational principle due to Reissner[9] forms the basis of the following development, which is obtained via the Hellinger-Reissner-Washizu formulation.[10] This formulation is particularly convenient for obtaining the structural equations in state vector form. The state vector equations obtained with this approach possess a natural decomposition that is quite useful for numerical solutions.

For the static equilibrium problem, the variational formulation can be written as (see Nomenclature)

$$\delta \int_0^{\ell} \mathfrak{U}[x, y(x), y'(x)]\,dx = 0 \tag{1}$$

from which the Euler-Lagrange equations of the variation are

$$-\frac{d}{dx}\frac{\partial \mathfrak{U}}{\partial y'} + \frac{\partial \mathfrak{U}}{\partial y} = 0 \tag{2}$$

The above formulation is applicable to either linear or nonlinear problems; the following analysis, however, will pursue only the solution of linear aeroelastic equations. Linearization of equations about a nonlinear steady-state solution introduces additional terms not discussed in this presentation. Nonetheless, the basic development given here remains valid for the solution of these linearized problems.

When linearity is invoked, and when it is assumed that the material constitutive relations can be specified, it is then possible to express the functional $\mathfrak{U}$ in the following convenient form:

$$\mathfrak{U} = y'^{T}\boldsymbol{D}y - \tfrac{1}{2}y^{T}\boldsymbol{K}y + \boldsymbol{p}^{T}y \tag{3}$$

where $\boldsymbol{K}$ is a spatially variable symmetric matrix containing the structural relations, $\boldsymbol{p}$ contains the external loads, and $\boldsymbol{D}$ is defined such that $(\boldsymbol{D}-\boldsymbol{D}^{T})$ is a constant skew-symmetric matrix with unit elements. The state vector y is specified in the form

$$y = \{y_F\, y_D\}^{T} \tag{4}$$

where y_F are generalized forces and y_D generalized displacements. This form for y is the same as would appear in a transfer matrix structural solution based upon a "mixed" finite-element force-displacement relationship. (The precise structure and content of the terms appearing in the above representation of the functional $\mathfrak{U}$ will be more apparent as we examine in a subsequent section a specific example for an anisotropic beam.) Now substituting Eq. (3) into Eq. (2) and performing the indicated differentiation yields the equilibrium equations

$$-\boldsymbol{J}y' - \boldsymbol{K}y + \boldsymbol{p} = 0 \tag{5}$$

in which

$$\boldsymbol{J} = \boldsymbol{D} - \boldsymbol{D}^{T} = \begin{bmatrix} 0 & -I \\ I & 0 \end{bmatrix} \tag{6}$$

Noticing that

$$\boldsymbol{J}^{-1} = \boldsymbol{J}^{T} = -\boldsymbol{J} \tag{7}$$

we can write the equations in the standard state vector form

$$y' = \boldsymbol{Z}y - a \tag{8}$$

where

$$\boldsymbol{Z} = \boldsymbol{J}\boldsymbol{K} \quad \text{and} \quad a = \boldsymbol{J}\boldsymbol{p} \tag{9}$$

Aeroelastic Equations

Since aeroelastic problems are characterized by their displacement dependent loading, Eq. (8) is modified by the usual procedure of breaking the total external loads acting on the system into a summation of those loads that act on a rigid structure plus perturbation loads due to elastic deformation. Therefore, for static aeroelastic problems, we now rewrite Eq. (8) as

$$y' = \boldsymbol{Z}y - qAy - a_r, \qquad y = y(x) \tag{10}$$

where q is the dynamic pressure and A is developed from an aerodynamic influence relationship. In fact, for the discrete version of this system, for which an example will be presented in a following section, A contains terms from an inverse aerodynamic influence matrix. Additionally, if A is partitioned corresponding to the force and displacement subsets of the state vector, only one of its submatrices contains nonzero elements, namely, that submatrix providing forces due to displacement.

Equations describing dynamic aeroelastic systems can be derived by additionally defining expressions for kinetic energy and any nonconservative forces acting on the system. Application of the extended Hamilton's principle then yields

dynamical equations from which we immediately remove time dependence by Laplace transformation. Following this procedure and then dropping nonhomogeneous load terms provides the equations suitable for aeroelastic stability analysis

$$\frac{\mathrm{d}}{\mathrm{d}x}\hat{y}=Z\hat{y}+s^2M\hat{y}+sC\hat{y}-Q(s,q)\hat{y}, \quad \hat{y}=\hat{y}(x,s) \tag{11}$$

in which M, C, and Q represent, respectively, the mass, damping, and unsteady aerodynamic terms. Again it can be noted that these terms contain only one nonzero submatrix when partitioned according to force and displacement subsets of the state vector.

Anisotropic Beam Equations

A simple anisotropic plate-beam model (Fig. 1) suitable for analyzing aeroelastic phenomena of large-aspect-ratio lifting surfaces is presented here to help clarify the foregoing formulation. Equations will be developed for sections taken normal to the structural reference axis. This model, which will be used in numerical examples, employs the assumptions used by Weisshaar[4,5] to describe laminated composite box-beam lifting surfaces for the purpose of aeroelastic analysis. The reader is referred as well to Jones[11] for development of the stiffness and compliance terms of laminated composite plates.

It is found that by using the composite plate compliance matrices A^*, B^*, and D^* and including transverse shear V_x the functional in the form required by Eq. (1) can be expressed as

$$\mathfrak{U}=\int_{-c/2}^{c/2}[n^T\epsilon^0+m^T\kappa-\tfrac{1}{2}(n^TA^*n+n^TB^*m+m^TB^*n$$

$$+m^TD^*m+\beta_sV_x^2-2V_x\gamma)]\mathrm{d}y+p_uu+p_\gamma\gamma+p_ww+p_\alpha\alpha \tag{12}$$

where an integration is to be performed over the chord length of the structural box. By assuming that other stresses are negligible compared to the direct stress in the spanwise direction and by assuming that chordwise deformations are also negligible, the stress and moment resultants can be approximated as

$$n=\{N_x \ 0 \ 0\}^T, \quad m=\{M_x \ 0 \ M_{xy}\}^T \tag{13}$$

and the in-plane strains and curvatures are approximated by

$$\epsilon^0=\{u_0' \ 0 \ 0\}^T, \quad \kappa=\{(\gamma'+y\alpha'') \ 0 \ 2\alpha'\}^T \tag{14}$$

Substituting Eqs. (13) and (14) into Eq. (12) and performing the indicated integration yields an expression from which the state vector and other terms appearing in Eq. (3) can be defined readily.

It is convenient at this point to introduce a nondimensional version of the resulting anisotropic beam equations. The nondimensional differential equations, in the form of Eq. (8), can be written as

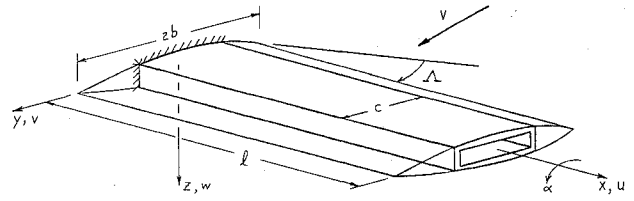

Fig. 1 Geometry for composite plate-beam model.

where

$$\bar{x}=x/\ell, \quad \bar{u}=u/\ell, \quad \bar{w}=w/\ell \tag{16}$$

It is also convenient to define

$$(EI)_R=c_RD_{11R} \tag{17}$$

which is the reference bending stiffness in terms of the appropriate composite stiffness. In terms of the reference bending stiffness, other nondimensional parameters appearing in Eq. (15) are the force and moment resultants and external loads

$$\bar{N}_x=\frac{c\ell^2N_x}{(EI)_R}, \quad \bar{M}_x=\frac{c\ell M_x}{(EI)_R}, \quad \bar{V}_x=\frac{c\ell^2V_x}{(EI)_R}, \quad \bar{M}_{xy}=\frac{c\ell M_{xy}}{(EI)_R}$$

$$\bar{p}_u=\frac{\ell^3p_u}{(EI)_R}, \quad \bar{p}_\gamma=\frac{\ell^2p_\gamma}{(EI)_R}, \quad \bar{p}_w=\frac{\ell^3p_w}{(EI)_R}, \quad \bar{p}_\alpha=\frac{\ell^2p_\alpha}{(EI)_R} \tag{18}$$

and the nondimensional composite compliances,

$$\bar{A}_{11}^*=\frac{(EI)_RA_{11}^*}{c\ell^2}, \quad \bar{B}_{11}^*=\frac{(EI)_RB_{11}^*}{c\ell}, \quad \bar{B}_{13}^*=\frac{(EI)_RB_{13}^*}{2c\ell}$$

$$\bar{D}_{11}^*=\frac{(EI)_RD_{11}^*}{c}, \quad \bar{D}_{13}^*=\frac{(EI)_RD_{13}^*}{2c}, \quad \bar{D}_{33}^*=\frac{(EI)_RD_{33}^*}{4c} \tag{19}$$

and, finally, the nondimensional shear compliance,

$$\bar{S}^*=(EI)_R\beta_s/\ell^2 \tag{20}$$

In regard to the aeroelastic equations (10) and (11), the load terms (i.e., inertia, damping, and aerodynamic) are made nondimensional in the same manner as the loads in Eq. (15). Additional details on the preceding development can be found in Lehman.[12]

Solution by Integrating Matrices

A numerical solution of the two-point boundary-value problems posed by the aeroelastic equations (10) and (11) and

$$\frac{\mathrm{d}}{\mathrm{d}\bar{x}}\begin{Bmatrix}\bar{N}_x\\ \bar{M}_x\\ \bar{V}_x\\ 2\bar{M}_{xy}\\ \bar{u}\\ \gamma\\ \bar{w}\\ \alpha\end{Bmatrix}=\begin{bmatrix}0 & 0 & 0 & 0 & 0 & 0 & 0 & 0\\ 0 & 0 & 1 & 0 & 0 & 0 & 0 & 0\\ 0 & 0 & 0 & 0 & 0 & 0 & 0 & 0\\ 0 & 0 & 0 & 0 & 0 & 0 & 0 & 0\\ \bar{A}_{11}^* & \bar{B}_{11}^* & 0 & \bar{B}_{13}^* & 0 & 0 & 0 & 0\\ \bar{B}_{11}^* & \bar{D}_{11}^* & 0 & \bar{D}_{13}^* & 0 & 0 & 0 & 0\\ 0 & 0 & \bar{S}^* & 0 & 0 & -1 & 0 & 0\\ \bar{B}_{13}^* & \bar{D}_{13}^* & 0 & \bar{D}_{33}^* & 0 & 0 & 0 & 0\end{bmatrix}\begin{Bmatrix}\bar{N}_x\\ \bar{M}_x\\ \bar{V}_x\\ 2\bar{M}_{xy}\\ \bar{u}\\ \gamma\\ \bar{w}\\ \alpha\end{Bmatrix}-\begin{Bmatrix}\bar{p}_u\\ \bar{p}_\gamma\\ \bar{p}_w\\ \bar{p}_\alpha\\ 0\\ 0\\ 0\\ 0\end{Bmatrix} \tag{15}$$

their boundary conditions can be formulated by an adaptation of the integrating matrix techniques presented by Vakhitov,[13] Hunter,[14] and White and Malatino.[15] The integrating matrix approach, which belongs to a class of collocation methods, is particularly convenient for solving the state vector form of equations presented here since only a single application of the integrating matrix is required. To formulate a solution, the integrating matrix will be applied as an operator in order to produce a discretized form of the aeroelastic equations. Reference 12 contains a more detailed discussion of integrating matrices, including a newly derived integrating matrix based upon Jacobi polynomials. The "Jacobi" integrating matrix can be applied to the solution of problems in the same manner as described by Hunter[14] for a "Newton" integrating matrix, which is derived from a Newton forward-difference interpolation formula. It will be assumed in what follows that the integrating matrix is applied only to analytic functions. For problems that possess discontinuities, a simple approach discussed by Vakhitov in Ref. 13 can be used to break the solution at the point of discontinuity and separate it into analytic regions.

Discrete Form of Aeroelastic Equations

Consider first a dimensionless form of the static aeroelastic equation (10) which must hold for any value of the spatial coordinate. Writing this equation at a discrete set of n points yields

$$\tilde{y}' = \tilde{Z}\tilde{y} - \lambda\tilde{A}\tilde{y} - \tilde{a}_r \tag{21}$$

where, for example

$$\tilde{y}^T = \{y_0^T \; y_1^T \ldots y_n^T\} \tag{22}$$

and

$$\lambda = \frac{2qb_R\ell^3\cos^2\Lambda}{(EI)_R}$$

At each of the n discrete points, the vector that is a solution of Eq. (10), and thus a component of Eq. (22), is defined to be a "local state vector." The ordering of components is arbitrary in the "global state vector" defined by Eq. (22). Therefore, for reasons of convenience, it is assumed in what follows that the global vector is reordered such that its structure is identical to that of the local vectors [i.e., it is partitioned into generalized force and displacement subsets identical to Eq. (4) and has "degrees-of-freedom" for each state variable grouped together]. An integrating matrix $\tilde{L}$, as developed by Hunter, is now applied as an operator to Eq. (21) resulting in

$$\tilde{y} = \tilde{L}\tilde{Z}\tilde{y} - \lambda\tilde{L}\tilde{A}\tilde{y} - \tilde{L}\tilde{a}_r + \tilde{k} \tag{23}$$

where $\tilde{k}$ is a constant vector of integration to be determined from boundary conditions. Once $\tilde{k}$ has been determined, we are left with a matrix eigenvalue problem if the nonhomogeneous terms are dropped, or a system of simultaneous equations if they are retained.

From this point on, cantilever boundary conditions will be assumed, for which the generalized displacement variables are zero at the fixed end and the generalized forces are zero at the free end. Employing this assumption to solve for $\tilde{k}$ in a manner similar to that of Ref. 14 allows Eq. (23) to be written in the form

$$[H - \lambda F\tilde{A}]\tilde{y} = f \tag{24}$$

where

$$H = I + F\tilde{Z} \tag{25}$$

$$F = [\tilde{B} - I]\tilde{L} \tag{26}$$

$$f = F\tilde{a}_r \tag{27}$$

and $\tilde{B}$ is a simple boundary condition matrix of the form specified in Ref. 14. Other types of homogeneous boundary conditions can be carried through with essentially the same result.

Equation Reduction by Partitioning

Rather than obtaining solutions for the entire matrix problem defined by Eq. (24), it is desirable to reduce the order by half and solve a corresponding system written in terms of displacement variables only. In fact, half of the information contained in Eq. (24) simply expresses constraint relationships. This can be easily verified by solving for the eigenvalues of the homogeneous form of Eq. (24), in which case half of the eigenvalues are zero. Thus, writing out the partitioned form of the matrices in Eq. (24) reveals that

$$H = \begin{bmatrix} H_{FF} & 0 \\ H_{DF} & H_{DD} \end{bmatrix}, \quad \tilde{A} = \begin{bmatrix} 0 & A_{FD} \\ 0 & 0 \end{bmatrix}$$

$$F = \begin{bmatrix} [B_n - I]L & 0 \\ 0 & -L \end{bmatrix} = \begin{bmatrix} L^* & 0 \\ 0 & -L \end{bmatrix}, \quad f = \begin{Bmatrix} L^*\tilde{a}_{r_F} \\ 0 \end{Bmatrix} \tag{28}$$

The H matrix, which contains only structural information, can be demonstrated to be nonsingular. Equation (24) can therefore be multiplied through by the inverse of H. As a consequence of this, in conjunction with the partitioned forms in Eq. (28), it can be shown that the reduced aeroelastic lift distribution problem is represented by

$$[I - \lambda TA_{FD}]\tilde{y}_D = T\tilde{a}_{r_F} \tag{29}$$

where

$$T = -H_{DD}^{-1}H_{DF}H_{FF}^{-1}L^* \tag{30}$$

In addition, the aeroelastic divergence eigenproblem is provided by the homogeneous portion of Eq. (29)

$$[TA_{FD} - (1/\lambda)I]\tilde{y}_D = 0 \tag{31}$$

Beginning with Eq. (11) and following a similar line of reasoning leads to a reduced flutter eigenproblem in the Laplace domain

$$\{I + T[M_{FD}s^{*2} + C_{FD}s^* - Q_{FD}(s^*,\lambda)]\}\tilde{y}_D = 0 \tag{32}$$

where

$$s^* = s\ell^2\sqrt{m_R/(EI)_R}$$

The actual computation of the coefficient matrices appearing in Eqs. (29-32) is in fact much simpler than it appears at first glance since the calculations involved are analytically reducible to a small number of simple operations on matrices that have an order equal only to the number of discretization points. The analytical reduction can readily be carried out since H_{DD} and H_{FF} are both very sparse and have block matrix form, rendering their inversion process trivial, These properties are due in part to the natural structure of the H matrix, aided by the convenient ordering of the global state vector. This is perhaps best described by an example that will later be used in flutter calculations.

Flutter Formulation

Considering the anisotropic beam examined earlier, we find that

$$H_{FF}=\begin{bmatrix} I & 0 & 0 & 0 \\ 0 & I & L^* & 0 \\ 0 & 0 & I & 0 \\ 0 & 0 & 0 & I \end{bmatrix}, \quad H_{DD}=\begin{bmatrix} I & 0 & 0 & 0 \\ 0 & I & 0 & 0 \\ 0 & L & I & 0 \\ 0 & 0 & 0 & I \end{bmatrix} \tag{33}$$

Anticipating assumptions that will later be made in the numerical flutter analyses (for the sole purpose of simplifying the presentation), we first assume that the $\bar{B}^*_{ij}$ coupling terms in Eq. (15) are zero and that transverse shear effects are negligible. Then inverting the matrices in Eq. (33), which simply involves taking the negative of the off-diagonal block, and using the result in Eq. (30) leads to

$$T=\begin{bmatrix} L\,\bar{A}^*_{11}L^* & 0 & 0 & 0 \\ 0 & L\,\bar{D}^*_{11}L^* & -L\,\bar{D}^*_{11}L^{*2} & L\,\bar{D}^*_{13}L^* \\ 0 & -L^2\,\bar{D}^*_{11}L^* & L^2\,\bar{D}^*_{11}L^{*2} & -L^2\,\bar{D}^*_{13}L^* \\ 0 & L\,\bar{D}^*_{13}L^* & -L\,\bar{D}^*_{13}L^{*2} & L\,\bar{D}^*_{33}L^* \end{bmatrix} \tag{34}$$

If it is further assumed that the lifting surface to be analyzed is unswept ($\Lambda=0$) and nonrotating and that strip theory unsteady aerodynamics is applicable, then a suitable description of the aerodynamic and mass terms in Eq. (32) would be

$$M_{FD}=\begin{bmatrix} 0 & 0 & 0 & 0 \\ 0 & 0 & 0 & 0 \\ 0 & 0 & \bar{m}_{ww} & \bar{m}_{w\alpha} \\ 0 & 0 & \bar{m}_{w\alpha} & \bar{m}_{\alpha\alpha} \end{bmatrix} \tag{35}$$

$$Q_{FD}(s^*,\lambda)=\begin{bmatrix} 0 & 0 & 0 & 0 \\ 0 & 0 & 0 & 0 \\ 0 & 0 & \hat{\mathfrak{L}}_w & \hat{\mathfrak{L}}_\alpha \\ 0 & 0 & \hat{\mathfrak{M}}_w & \hat{\mathfrak{M}}_\alpha \end{bmatrix}$$

where

$$\bar{m}_{ww}=\bar{m}, \quad \bar{m}_{w\alpha}=\bar{m}\left(\frac{b_R}{\ell}\right)\bar{\chi}_\alpha, \quad \bar{m}_{\alpha\alpha}=\bar{m}\left(\frac{b_R}{\ell}\right)^2\bar{r}^2_\alpha \tag{36}$$

The strip theory aerodynamic terms are as defined by Housner and Stein,[16] with the exception that here they are made applicable to the Laplace domain by inclusion of either the generalized Theodorsen's function or an appropriate rational approximation.[17-19] If structural damping is now neglected, it can easily be shown that with the specified assumptions the flutter eigenvalue problem represented by Eq. (32), along with Eqs. (34-36), can be reduced to

$$\begin{bmatrix} (I+G_{33}) & G_{34} \\ G_{43} & (I+G_{44}) \end{bmatrix}\begin{Bmatrix} \bar{w} \\ \alpha \end{Bmatrix}=0 \tag{37}$$

where

$$G=T[M_{FD}s^{*2}-Q_{FD}(s^*,\lambda)] \tag{38}$$

Equation (37) can be numerically evaluated for the roots loci of the aeroelastic modes as a function of the dynamic pressure parameter λ, with instability being associated with complex roots s^* that have positive real parts. It has been found that this approach provides a very efficient and convenient method for performing rapid flutter analyses.

Numerical Examples

Several sample problems are presented to verify the methods developed in this paper and to assess the accuracy of the integrating matrix solutions. As will be noted, these simplified problems have either analytical or alternate numerical solutions that will provide a basis for comparison with the state vector approach. In the following discussions it should also be noted that the number of discretization intervals is one less than the number of discretization points. Additionally, the integrating matrices employed here always use the maximum-order polynominal that can be represented by the given number of discretization points.

With regard to numerical procedures, all eigenvalue calculations for the nonsymmetric matrix eigenproblem of Eq. (31) utilize a double-precision EISPACK[20] routine for real nonsymmetric matrices. For flutter solutions, complex roots of Eq. (37) are evaluated by a determinant search routine that employs Muller's method. All of the numerical calculations were performed on an IBM 370/168.

Divergence and Lift for an Unswept Isotropic Wing

For the case of strip theory aerodynamics, solutions for torsional divergence and aeroelastic lift distribution of unswept, cantilevered, isotropic wings can be obtained by solving a second-order differential equation describing the torsional equilibrium of the wing.[21] The state vector form of this equation and the accompanying parameters are presented in the Appendix. Despite its simple nature, this problem provides a very good test for the convergence and accuracy characteristics of the integrating matrix solution of the state vector equations and will be used here to compare the Jacobi and Newton integrating matrix solutions.

In Table 1, the nondimensional divergence dynamic pressure of a uniform wing is given for both Jacobi and Newton integrating matrix solutions as the number of discretization intervals varies. Results are compared with the exact solutions developed in Ref. 21. As indicated by the error between the approximate and exact solutions, the convergence to the lower eigenvalues is quite rapid, with the Jacobi results being obviously superior in this regard. For either type of integrating matrix, very good accuracy is obtained with surprisingly few discretization points. Since practical divergence calculations require only the lowest eigenvalue, sufficient accuracy for most purposes is obtained with as few as three intervals.

Table 2 presents results similar to Table 1 for the nondimensional divergence dynamic pressure of a linearly tapered wing with a taper ratio of one-half. Again, convergence to the lowest eigenvalues is quite good for both Jacobi and Newton integrating matrix solutions, with the Jacobi solutions converging most rapidly to the lowest eigenvalue. As should be expected, however, the convergence is not as fast as for the uniform-wing example.

It should be noted that the solutions in Tables 1 and 2 present all of the available eigenvalues for a given level of discretization. As with any discrete solution, the higher eigenvalues are increasingly less accurate. By comparing the Jacobi and Newton solutions, one can readily see that the highest eigenvalues of the Jacobi solutions are actually further from the exact results than the corresponding Newton solutions. On the other hand, the Jacobi solutions converge more rapidly than the Newton solutions as each new discretization point is added. In contrast with the Jacobi solutions, the Newton solutions for the uniform wing exhibit

Table 1 Torsional divergence eigenvalues ν for an unswept isotropic wing with $\beta = 0.0$

No. of intervals	Mode	Jacobi	Newton	Exact	% Error Jacobi	% Error Newton
2	1	1.582576	1.582576	1.570796	0.749938	0.749938
	2	7.582580	7.582580	4.712389	60.9073	60.9073
3	1	1.571009	1.569703	1.570796	0.013560	−0.069583
	2	4.962687	4.826099	4.712389	5.31149	2.41300
	3	15.39166	14.25626	7.853982	95.9727	81.5163
4	1	1.570799	1.570732	1.570796	0.000191	−0.004074
	2	4.735692	4.665351	4.712389	0.494505	−0.998177
	3	8.807365	8.070704	7.853982	12.1388	2.75939
	4	25.64255	21.64282	10.99557	133.208	96.8321
5	1	1.570797	1.570803	1.570796	0.000064	0.000446
	2	4.713869	4.706141	4.712389	0.031407	−0.132587
	3	8.011505	7.631141	7.853982	2.00564	−2.83730
	4	13.27345	11.23810	10.99557	20.7163	2.20567
	5	38.40523	29.57599	14.13717	171.661	109.207

Table 2 Torsional divergence eigenvalues ν for an unswept isotropic wing with $\beta = 0.5$

No. of intervals	Mode	Jacobi	Newton	Exact	% Error Jacobi	% Error Newton
2	1	1.613095	1.613095	1.652805	−2.40258	−2.40258
	2	11.15869	11.15869	3.627852	207.584	207.584
3	1	1.643238	1.665064	1.652805	−0.578834	0.741709
	2	3.587127	3.535655	3.627852	−1.12257	−2.54137
	3	22.39381	20.38371	5.807501	285.601	250.989
4	1	1.652913	1.649068	1.652805	0.006534	−0.226100
	2	3.580021	3.658788	3.627852	−1.31844	0.852736
	3	6.040474	5.622661	5.807501	4.01159	−3.18278
	4	37.76820	30.95097	8.215935	359.694	276.719
5	1	1.652826	1.653185	1.652805	0.001271	0.022991
	2	3.633674	3.608995	3.627852	0.160481	−0.519784
	3	5.721657	5.887524	5.807501	−1.47816	1.37793
	4	9.001691	7.591113	8.215935	9.56381	−7.60500
	5	57.31683	42.52789	10.27790	457.671	313.780

Table 3 Normalized elastic lift distribution at specified spanwise points[a] for an unswept, isotropic wing with $\beta = 0.5$ ($\nu = 0.5\nu_{\mathrm{Div},\beta=0}$)

No. of points	Point	C_{L_e}/C_{L_r} Jacobi	C_{L_e}/C_{L_r} Exact	% Error
3	1	1.000000	1.000000	—
	2	1.265245	1.240130	2.02516
	3	1.422478	1.435794	−0.927431
4	1	1.000000	1.000000	—
	2	1.124033	1.126779	−0.243650
	3	1.358704	1.352918	0.427661
	4	1.435765	1.435794	−0.002083
5	1	1.000000	1.000000	—
	2	1.077568	1.077168	0.037079
	3	1.239274	1.240130	−0.069041
	4	1.398306	1.397425	0.063030
	5	1.435797	1.435794	0.000160
6	1	1.000000	1.000000	—
	2	1.051681	1.051741	−0.005676
	3	1.167149	1.167017	0.011311
	4	1.313242	1.313421	−0.013644
	5	1.416360	1.416229	0.009264
	6	1.435793	1.435794	−0.000105

[a] The Jacobi integrating matrix collocation points are the same as Lobatto quadrature points.

an oscillatory convergence character. From a practical point of view, however, both Jacobi- and Newton-based solutions are capable of providing accurate results with a relatively small amount of discretization.

Presented in Table 3 are results comparing approximate and exact solutions for the ratio of elastic to rigid lift distribution for an isotropic wing with a taper ratio of one-half. The approximate results were obtained using the Jacobi matrix, and the dynamic pressure parameter was specified to be one-half the divergence value for a uniform wing. As in the preceding examples, the accuracy proves to be very good for a relatively small number of points.

Lift Distribution for a Uniform Composite Wing

To verify the state vector solution approach for anisotropic composite wings, a sample problem was investigated using the composite wing examined by Weisshaar in Ref. 4. Aerodynamic loads were calculated from simple strip theory. Figure 2 displays the results obtained by this author for the maximum and minimum values of normalized elastic lift distribution for a uniform, swept-forward, composite wing with all fibers oriented at an angle θ with respect to the structural reference axis. These results correspond to the maximum load amplification and attenuation that can be achieved by orienting the reinforcing fibers. Hence, these solutions are an indicator of the maximum amount of

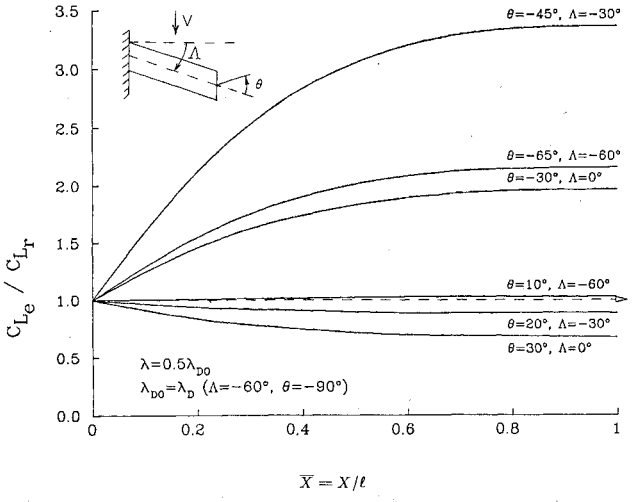

Fig. 2 Normalized elastic lift distribution for uniform composite wing at selected values of fiber orientation and forward sweep angle.

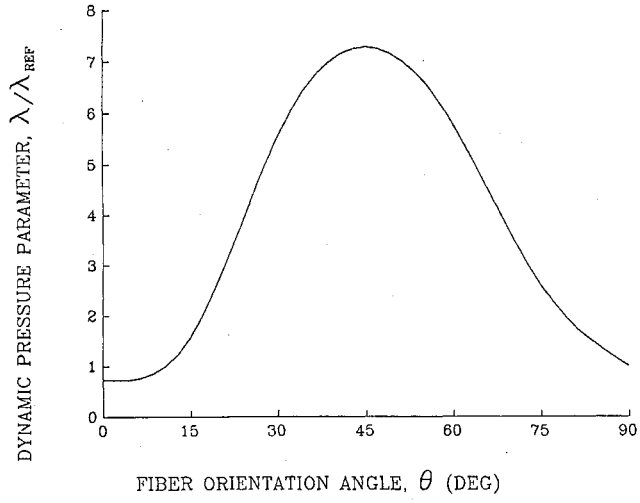

Fig. 3 Effect of fiber orientation on flutter dynamic pressure for an unswept, uniform composite wing ($\lambda_{REF} = 1.214$, bending-twist coupling neglected).

"tailoring" that can be achieved for a given configuration and material. It is interesting to note that the maximum amount of lift attenuation, which also corresponds to maximum divergence speed, occurs when the fibers are oriented ahead of the structural reference axis. Those swept-forward wings whose lift distributions fall below the dashed rigid wing reference line are in fact displaying the load-alleviating property typical of isotropic swept-back wings. These results are verified by an analytical solution developed in Ref. 5 for normalized elastic lift distribution of uniform composite wings. A comparison of the analytical lift distribution solutions with the approximate Jacobi integrating matrix solutions obtained using five discretization intervals shows a maximum deviation from the true lift distribution curves of less than 0.1%.

Flutter of Isotropic and Composite Wings

Initial flutter calculations were verified through comparison with analytical solutions obtained by Goland[22] for an unswept isotropic wing (with corrections in Goland and Luke[23]). Table 4 compares numerical flutter results using Eqs. (37) and (38) with those of Goland and with a numerical solution of Housner and Stein given in Ref. 16. The accuracy of the state vector method appears extremely good for a very small number of discretization points. It should also be

Table 4 Flutter velocity for an unswept, uniform, isotropic wing

Solution	Description	Flutter velocity, km/h
Refs. 22, 23	Exact analysis	494
Ref. 16	25 finite-difference points	483.1
State vector	Jacobi I.M., 2 intervals	486.0
State vector	Jacobi I.M., 3 intervals	494.4
State vector	Jacobi I.M., 4 intervals	494.4

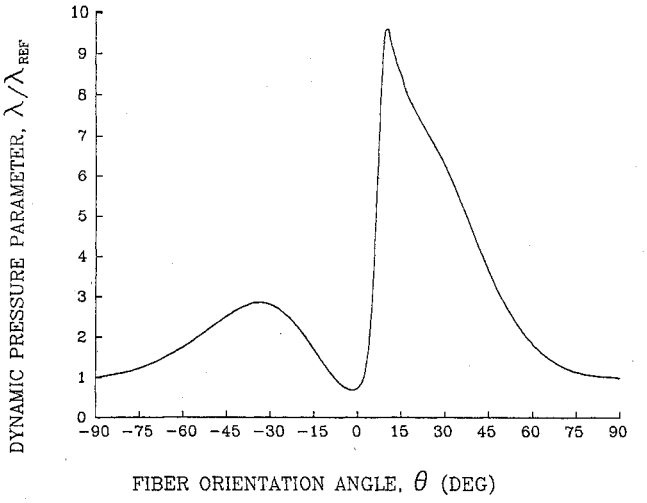

Fig. 4 Effect of fiber orientation on flutter dynamic pressure for an unswept, uniform composite wing ($\lambda_{REF} = 1.214$, bending-twist coupling included).

pointed out that the unsteady strip theory aerodynamic calculations used in this comparison employ a rational approximation of the Theodorsen function due to R. T. Jones as discussed in Ref. 17.

A second example allowing additional verification of the flutter calculations is presented in Fig. 3, which displays the variation in nondimensional flutter dynamic pressure λ as a function of the fiber orientation angle θ in an unswept uniform cantilever wing. These results, which are for a wing with an aspect ratio of 6.67 and mass ratio μ of 8.0, have been normalized to unity at a fiber angle of $\theta = 90$ deg ($\lambda_{REF} = 1.214$). The simplified composite layup assumed here has all fibers oriented in a single direction, which is a special case of a midplane symmetric angle-ply laminate. This example is taken from Housner and Stein[16] and results here compare very closely with Fig. 9 of that reference. One should carefully note, however, that this example assumes no bending-twist coupling ($\bar{D}^*_{13} = 0$) for the composite material. Therefore, as could be anticipated, the flutter speed follows the torsional stiffness variation, giving a flutter speed maximum at θ equal to 45 deg.

Plotted in Fig. 4 is the nondimensional flutter dynamic pressure variation for the same wing with inclusion of the composite bending-twist coupling term. Note that the coupling term is periodic over 180 deg. Comparing the flutter dynamic pressures in Figs. 3 and 4 for the range of θ of 0-90 deg reveals a strong effect inherent in the coupling term. It should be emphasized, however, that the simplified composite layup assumed here, with all fibers in the same direction, will produce maximum coupling and therefore a limiting result. A practical layup with fibers in other directions tends more toward quasi-isotropic behavior, which quickly reduces the relative effect of the coupling term. The effect of this relative reduction in coupling will be to smooth out somewhat the sharp peaks and rapid changes that are evident in Fig. 4.

Conclusion

This paper has presented a state vector formulation of the linear ordinary differential equations describing both static and dynamic aeroelastic behavior of moderate-to-high-aspect-ratio lifting surfaces. Application of an integrating matrix to the state vector equations produces a set of matrix equations to be solved for aeroelastic response and stability. As a result of the special structure of these matrix equations, they can be manipulated and simplified to provide an efficient, easily coded, computational approach, even when anisotropic material behavior is present. Several simplified examples have demonstrated how this method can be applied to aeroelastic problems and have shown that very good solution accuracies can be obtained. The formulation and techniques presented here are quite general and can be extended to solve other more difficult aeroelastic problems, including those for rotating lifting surfaces.

Appendix: Torsional Equations of an Isotropic Wing

The nonhomogeneous aeroelastic equilibrium equation for torsion of an unswept, linearly tapered, isotropic, cantilevered wing is given in Ref. 21. In nondimensional form it appears as

$$(\tau\alpha')' + \nu^2\alpha = \nu^2\alpha_0 \tag{A1}$$

with boundary conditions given by

$$\alpha(0) = 0, \qquad \tau\alpha'(1) = 0 \tag{A2}$$

The parameters appearing in Eq. (A1) are

$$\tau = GJ/GJ_R, \quad \nu^2 = \nu_R^2(1-\beta\bar{x})^2, \quad GJ = GJ_R(1-\beta\bar{x})^4 \tag{A3}$$

$$\nu_R^2 = 2qb_R e_R \alpha_0 / GJ_R \tag{A4}$$

and the taper ratio is $(1-\beta)$. The homogeneous form of Eq. (A1) is a Sturm-Liouville problem. For a unit value of the root angle of attack, Eq. (A1) can be written in state vector form as

$$\frac{\mathrm{d}}{\mathrm{d}\bar{x}}\begin{Bmatrix}\tau\alpha'\\ \alpha\end{Bmatrix} = \begin{bmatrix}0 & 0\\ 1/\tau & 0\end{bmatrix}\begin{Bmatrix}\tau\alpha'\\ \alpha\end{Bmatrix} - \nu^2\begin{bmatrix}0 & 1\\ 0 & 0\end{bmatrix}\begin{Bmatrix}\tau\alpha'\\ \alpha\end{Bmatrix} - \begin{Bmatrix}\nu^2\\ 0\end{Bmatrix} \tag{A5}$$

The homogeneous form of Eq. (A5), with boundary conditions, defines the torsional divergence eigenvalue problem, whereas the nonhomogeneous form represents the simultaneous equations for lift distribution.

Acknowledgments

This research was supported in part by the National Aeronautics and Space Administration under Grant NGL-05-020-243, and in part by the Air Force Office of Scientific Research under Grant AFOSR 77-3263.

The research reported herein was conducted at Stanford University, Department of Aeronautics and Astronautics.

References

[1] Gimmestad, D., "An Aeroelastic Optimization Procedure for Composite High Aspect Ratio Wings," *AIAA/ASME/ASCE/AHS 20th Structures, Structural Dynamics and Materials Conference Proceedings*, Vol. I, April 1979, pp. 79-86.

[2] Diederich, F. W. and Budiansky, B., "Divergence of Swept Wings," NACA TN 1680, Aug. 1948.

[3] Diederich, F. W. and Foss, K. A., "Charts and Approximate Formulas for the Estimation of Aeroelastic Effects on the Loading of Swept and Unswept Wings," NACA TN 2608, Feb. 1952.

[4] Weisshaar, T. A., "Aeroelastic Stability and Performance Characteristics of Aircraft with Advanced Composite Sweptforward Wing Structures," AFFDL-TR-78-116, Sept. 1978.

[5] Weisshaar, T. A., "Forward Swept Wing Static Aeroelasticity," AFFDL-TR-79-3087, June 1979.

[6] Steele, C. R., "Asymptotic Solutions Without Special Functions for Steep and Shallow Shells," *Mechanics Today*, Vol. 5, 1980, pp. 483-494.

[7] Steele, C. R., Ranjan, C. V., and Pulliam, T. H., "Computer Analysis of Shells of Revolution Using Asymptotic Results," *AIAA/ASME/ASCE/AHS 20th Structures, Structural Dynamics and Materials Conference Proceedings*, Vol. I, April 1979, pp. 162-170.

[8] Steele, C. R. and Barry, K. E., "Asymptotic Integration Methods Applied to Rotating Beams," *Journal of Applied Mechanics*, Vol. 47, No. 4, Dec. 1980, pp. 884-890.

[9] Reissner, E., "On a Variational Theorem in Elasticity," *Journal of Mathematics and Physics*, Vol. 29, 1950, pp. 27-52.

[10] Reissner, E., "Variational Methods and Boundary Conditions in Shell Theory," *Studies in Optimization, Proceedings of the Symposium on Optimization*, Vol. I, Society for Industrial and Applied Mathematics, Philadelphia, Pa., 1970, pp. 78-94.

[11] Jones, R. M., *Mechanics of Composite Materials*, McGraw-Hill Book Co., New York, 1975, pp. 147-156.

[12] Lehman, L. L., "Hybrid State Vector Methods for Structural Dynamic and Aeroelastic Boundary Value Problems," Ph.D. Dissertation, Dept. of Aeronautics and Astronautics, Stanford University, Stanford, Calif., 1982 (to be available as a NASA contractor report, 1982).

[13] Vakhitov, M. B., "Integrating Matrices as a Means of Numerical Solution of Differential Equations in Structural Mechanics," *Izvestiya VUZ. Aviatsionnaya Tekhnika*, Vol. 9, No. 3, 1966, pp. 50-61 (English translation: *Soviet Aeronautics*, Vol. 9, No. 3, 1966, pp. 27-33).

[14] Hunter, W. F., "Integrating-Matrix Method for Determining the Natural Vibration Characteristics of Propeller Blades," NASA TN D-6064, Dec. 1970.

[15] White, W. F. Jr. and Malatino, R. E., "A Numerical Method for Determining the Natural Vibration Characteristics of Rotating Nonuniform Cantilever Blades," NASA TM X-72751, Oct. 1975.

[16] Housner, J. M. and Stein, M., "Flutter Analysis of Swept-wing Subsonic Aircraft with Parameter Studies of Composite Wings," NASA TN D-7539, Sept. 1974.

[17] Edwards, J. W., "Unsteady Aerodynamic Modeling and Active Aeroelastic Control," Stanford University, SUDAAR 504, Feb. 1977.

[18] Edwards, J. W., Ashley, H., and Breakwell, J. V., "Unsteady Aerodynamic Modeling for Arbitrary Motions," AIAA Paper 77-451, March 1977.

[19] Edwards, J. W., "Applications of Laplace Transform Methods to Airfoil Motion and Stability Calculations," *AIAA/ASME/ASCE/AHS 20th Structures, Structural Dynamics and Materials Conference Proceedings*, Vol. II, April 1979, pp. 465-481.

[20] Smith, B. T., et al., *Matrix Eigensystem Routines: EISPACK Guide*, Springer-Verlag, New York, 1974.

[21] Bisplinghoff, R. L., Ashley, H., and Halfman, R. L., *Aeroelasticity*, Addison-Wesley, Reading, Mass., 1955, pp. 431-448.

[22] Goland, M., "The Flutter of a Uniform Cantilever Wing," *Journal of Applied Mechanics*, Vol. 12, No. 4, Dec. 1945, pp. A-197-A-208.

[23] Goland, M. and Luke, Y. L., "The Flutter of a Uniform Wing with Tip Weights," *Journal of Applied Mechanics*, Vol. 15, No. 1, March 1948, pp. 13-20.